International Journal of Signal Processing, Image Processing and Pattern Recognition
Vol.9, No.6 (2016), pp.89-102
http://dx.doi.org/10.14257/ijsip.2016.9.6.08

Carrier Frequency Estimation with Cyclostationary Signals in Impulsive Noise

Yang Liu[1, 2], Yong Tie[1], Shun Na[1] and Shenglong Tan[1]

[1]*College of Electronic Information Engineering, Inner Mongolia University, Hohhot, 010021, China*
[2]*Faculty of Electronic Information and Electrical Engineering, Dalian University of Technology, Dalian, 116023, China*
[1]*yangliuimu@163.com*

Abstract

This paper addresses the estimation of carrier frequency for cyclostationary AM, BPSK, and QPSK signals in the presence of interfering signals and α-stable impulsive noise. The performance of conventional DFT algorithms suffers from severe degradation in impulsive noise environments. By fusing cyclostationarity and fractional lower-order statistics, we introduce a signal selective carrier frequency estimation algorithm for AM, BPSK, and QPSK signals. The new method exploits $_p$ th-order cyclostationarity property of signals in impulsive noise. Compared with the existing DFT algorithm, the new method is highly tolerant to interference, Gaussian and non-Gaussian impulsive noises. The performance of the new algorithm is studied using simulations in a variety of interference and noise conditions. Simulation results indicate that the proposed algorithm outperforms the conventional DFT method in impulsive noise.

Keywords: *Carrier frequency estimation, impulsive noise, fractional lower-order statistics, cyclostationarity*

1. Introduction

In dealing with channel estimation, most investigators assume zero frequency offset between the carrier and the local reference at the receiver. In practice, this means that the offset is so small that the demodulated signal incurs only negligible phase rotations during the preamble duration [1]. Nevertheless, in broadband wireless communication systems, it is highly possible to receive a signal with a large frequency offset, which caused the traditional carrier recovery loop invalid because of its limited frequency acquisition range [2-3]. In such conditions, a critical operation in the receiver is the estimation of the carrier frequency in order to perform accurate compensation in the demodulation process. This estimation process is generally performed directly on the received bandpass modulated signals.

One of the widely used large carrier frequency offset estimation methods is DFT algorithm, which is commonly employed in digital signal analysis instrumentation to guarantee that the residue carrier frequency offset within the capture bandwidth of the following carrier synchronization loop. A fast Fourier transform (FFT) algorithm to estimate carrier frequency deviation based on the maximum likelihood parameter estimation approach for QPSK was proposed in [4]. Although this method can estimate the carrier frequency directly, its estimation accuracy is low. In order to improve the frequency and phase resolution capabilities, an interpolation algorithm for carrier frequency estimation based on FFT in burst M-PSK communication system was presented in [5]. The problem over frequency flat fading channels has been investigated in [6], a feed-forward technique exploiting the

ISSN: 2005-4254 IJSIP

sample correlation function of the received signal was proposed. A class of frequency estimation algorithms intended for filter bank burst-mode multi-carrier transmission over time-frequency selectively fading channels was introduced in [7]. The Cramer-Rao lower bound (CRB) for the joint estimation of the carrier phase and frequency offset from a noisy linearly modulated burst signal containing random data symbols as well as known pilot symbols was presented in [8].

Many frequency estimation schemes have been proposed for the additive white Gaussian noise and frequency selective and flat fading channels. However, the assumption of Gaussian noise is often unrealistic. Studies and experimental measurements have shown that a broad and increasingly important class of noises such as underwater acoustic, atmospheric noise, multi-user interference and radar clutters in real world applications are non-Gaussian processes due mostly to impulsive phenomena [9]. It has been shown that α-stable distributions are more appropriate for modeling impulsive noise than Gaussian distribution in signal processing applications [10], which include the Gaussian process as a special case ($\alpha = 2$). This type of distribution provides attractive theoretical and applicable tools for many fields including communication, radar, sonar, *etc* [11]. The problem of parameter estimation in heavy-tailed noise coming from a symmetric α-stable ($S\alpha S$) distribution have been studied in [12], and several robust fractional lower-order statistics (FLOS) based methods have been developed. Although the FLOS based estimators are robust to both Gaussian and impulsive noise, the interferences which occupy the same spectral band as the SOI can severely degrade the performance of these methods. Looking toward real world applications, we are interested in developing carrier frequency estimation algorithms accounting for interference, Gaussian and non-Gaussian random processes.

Many man-made signals arising in communications, telemetry, radar and sonar applications exhibit cyclostationarity [13-14]. By exploiting this cyclostationarity property of such signals, several parameter estimation methods was introduced in [15].The signal-selective methods exploited the unique second-order cyclostationarity of the signal of interest (SOI), are inherent immune to interference and Gaussian noise. Most of the proposed cyclostationary methods assume that the noise is additive Gaussian noise. However, the assumption of Gaussian noise is often unrealistic. In this paper, we address the problem of carrier frequency estimation for cyclostationary signals in the presence of interference and impulsive noise. In order to alleviate the problems of impulsive noise and interference, we introduce an approach to exploit cyclostationarity of signals with fractional lower-order cyclic statistics. We then propose a robust signal-selective algorithm for AM, BPSK, and QPSK signals. The proposed algorithm takes advantages of signal-selective methods and FLOS based methods, is robust against Gaussian noise, impulsive noise and interfering signals.

2. Problem Formulation

The signal model considered in this paper can be modeled as

$$x(t) = s(t)e^{j2\pi f_c t} + n(t) \tag{1}$$

where $x(t)$ is the signal at the receiver antenna, $s(t)$ is an equivalent lowpass signal of the receiver signal, and $n(t)$ is signal not of interest (SNOI) including interfering signals and independent receiver noise. For AM signal the $s(t)$ is a stationary random process. For linear modulation (PSK) signal the $s(t)$ is given by

$$s(t) = A_m g(t), \quad m = 1, 2, \ldots, M \tag{2}$$

where A_m is complex and equal to $e^{j\frac{2\pi}{M}(m-1)}$.

The definition of cyclic autocorrelation function at certain cycle frequency ε is defined as

$$R_x^{\varepsilon}(\tau) \equiv \left\langle x(t+\tau/2)x^*(t-\tau/2)e^{-j2\pi\varepsilon t} \right\rangle \tag{3}$$

where $\langle\cdot\rangle$ is time-averaging operation $\lim_{T\to\infty}(1/T)\int_{-T/2}^{T/2}(\cdot)dt$, and $*$ denotes the conjugate [13]. The cyclic spectrum $S_x^{\varepsilon}(f)$ is defined to be the Fourier transform of the cyclic autocorrelation

$$S_x^{\varepsilon}(f) \equiv \int R_x^{\varepsilon}(\tau)e^{-j2\pi f\tau}d\tau \tag{4}$$

However, the stable distribution variables possess finite *p*th-order moments only for $p<\alpha$ while $E[|X|^p]=\infty$ for all $p\geq\alpha$. When the received noises in $n(t)$ contains α-stable impulsive components in real world applications, the second-order correlation function $E[x(t+\tau)x(t)]$ will become infinite. As a result of this effect, cyclic autocorrelation and spectral correlation function will become unbounded.

$$R_x^{\varepsilon}(\tau) \equiv \lim_{T\to\infty}\frac{1}{T}\int_{-T/2}^{T/2}E[x(t+\tau)x(t)]e^{-j2\pi\varepsilon t}dt=\infty \tag{5}$$

$$S_x^{\varepsilon}(f) \equiv \int R_x^{\varepsilon}(\tau)e^{-j2\pi f\tau}d\tau=\infty \tag{6}$$

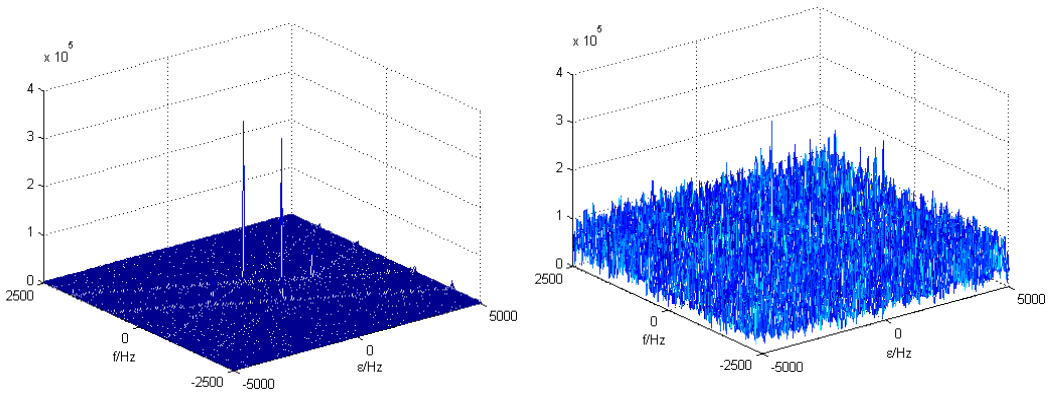

(a) Gaussian Noise ($\alpha=2$) (b) Impulsive Noise ($\alpha=1.8$)

Figure 1. Calculated Spectral Correlation Magnitudes for QPSK Signal in Gaussian and Impulsive Noises ($\alpha=1.8$)

Figure 1 shows the effects of $S\alpha S$ noise on the spectral correlation function of QPSK signal which has carrier frequency $f=0.1f_s$, and keying rate $\varepsilon=0.005f_s$. We notice that the spectral correlation function is immune to the Gaussian noise ($\alpha=2$), but it is completely masked by impulsive noise. Since cyclic correlation and spectrum are not defined for $\alpha<2$, conventional signal-selective and second-order statistics based DFT estimation methods can no longer be applied when the noise is impulsive.

3. Robust Carrier Frequency Estimation Algorithm

The conventional cyclostationarity is useless due to the unboundness of the cyclic correlation function and cyclic spectrum in $S\alpha S$ impulsive noise environments. By utilizing fractional lower-order statistics we introduce a new type cyclic statistics for exploiting periodicity in the presence of impulsive noise. Furthermore, we propose a signal-selective carrier frequency estimation algorithm for AM, BPSK, and QPSK signals.

It has been shown that PFLOM have been used in the design of signal processing algorithms to reduce impulsive effects [17-19]. The *p*th-order PFLOM is defined as

$$z^{\langle p \rangle} = |z|^{p-1} z \tag{7}$$

Equation (7) can be rewritten in a polar form, if $z = re^{j\theta}$, then it is easy to show that $z^{\langle p \rangle} = r^p e^{j\theta}$, so that the PFLOM acts only on the magnitude of its operand and preserves its phase. It is indicated that $z^{\langle p \rangle}$ has the same period as that of the z.

We can define a new type of cyclic statistics based on the *p*th-order PFLOM to exploit the periodicity of signals. Consider the random process $s(t)$, the *p*th-order cyclic correlation of $s(t)$ at cycle frequency ε is defined by

$$R_{s,p}^{\varepsilon}(\tau) \triangleq \left\langle s(t+\tau/2)[s^*(t-\tau/2)]^{\langle p-1 \rangle} e^{-j2\pi\varepsilon t} \right\rangle \tag{8}$$

where $1 < p < \alpha$. The *p*th-order cyclic spectrum is defined to be the Fourier transform of the *p*th-order cyclic correlation,

$$S_{s,p}^{\varepsilon}(f) = \int_{-\infty}^{\infty} R_{s,p}^{\varepsilon}(\tau) e^{-j2\pi f\tau} d\tau \tag{9}$$

The *p*th-order cycostationarity plays a role analogous to second-order cyclic statistics, where one of the input signals is $s(t)^{\langle p-1 \rangle}$. Consequently, *p*th-order cyclic statistics have some effects on suppressing impulsive noise.

In general, the AM signal can be expressed as

$$x(t) = a(t)\cos(2\pi f_c t + \theta) \tag{10}$$

where $a(t)$ is modeled as a zero-mean Gaussian process. The *p*th-order autocorrelation function of AM signal is given by

$$\begin{aligned} R_{x,p}(\tau) &= E\left(x(t+\tau/2)\left[x^*(t-\tau/2)\right]^{\langle p-1 \rangle}\right) \\ &= E[a(t+\tau/2)\cos(2\pi f_c(t+\tau/2)+\theta) \\ &\quad \times (a^*(t-\tau/2)\cos(2\pi f_c(t-\tau/2)+\theta))^{\langle p-1 \rangle}] \\ &= E(a(t+\tau/2)[a^*(t-\tau/2)]^{\langle p-1 \rangle}) \\ &\quad \times \cos(2\pi f_c(t+\tau/2)+\theta)\left[\cos(2\pi f_c(t-\tau/2)+\theta)\right]^{\langle p-1 \rangle} \end{aligned} \tag{11}$$

where

$$\begin{aligned} &\left[\cos(2\pi f_c(t-\tau/2)+\theta)\right]^{\langle p-1 \rangle} \\ &= \left|\cos(2\pi f_c(t-\tau/2)+\theta)\right|^{p-2} \cos(2\pi f_c(t-\tau/2)+\theta) \end{aligned} \tag{12}$$

It follows from (12) that

$$\begin{aligned} R_{x,p}(\tau) &= \left|\cos\left(2\pi f_c(t-\tau/2)+\theta\right)\right|^{p-2} E\left(a(t+\tau/2)\left[a^*(t-\tau/2)\right]^{\langle p-1\rangle}\right) \\ &\times \cos\left[2\pi f_c(t+\tau/2)+\theta\right]\cos\left[2\pi f_c(t-\tau/2)+\theta\right] \\ &= \frac{1}{4}\left|\cos\left(2\pi f_c(t-\tau/2)+\theta\right)\right|^{p-2} E\left(a(t+\tau/2)\left[a^*(t-\tau/2)\right]^{\langle p-1\rangle}\right) \\ &\times [e^{j2\pi f_c\tau} + e^{-j2\pi f_c\tau} + e^{j(4\pi f_c t+2\theta)} + e^{-j(4\pi f_c t+2\theta)}] \end{aligned} \tag{13}$$

By taking Fourier series transform, the Fourier coefficient is referred to as *p*th-order cyclic autocorrelation function,

$$\begin{aligned} R_{x,p}^{\varepsilon}(\tau) &= \frac{1}{4}C_p e^{i2\pi f_c\tau}\left\langle E\left(a(t+\tau/2)\left[a^*(t-\tau/2)\right]^{\langle p-1\rangle}\right)e^{-i2\pi\varepsilon t}\right\rangle \\ &+ \frac{1}{4}C_p e^{-i2\pi f_c\tau}\left\langle E\left(a(t+\tau/2)\left[a^*(t-\tau/2)\right]^{\langle p-1\rangle}\right)e^{-i2\pi\varepsilon t}\right\rangle \\ &+ \frac{1}{4}C_p e^{i\theta}\left\langle E\left(a(t+\tau/2)\left[a^*(t-\tau/2)\right]^{\langle p-1\rangle}\right)e^{-i2\pi(\varepsilon-2f_c)t}\right\rangle \\ &+ \frac{1}{4}C_p e^{-i\theta}\left\langle E\left(a(t+\tau/2)\left[a^*(t-\tau/2)\right]^{\langle p-1\rangle}\right)e^{-i2\pi(\varepsilon+2f_c)t}\right\rangle \end{aligned} \tag{14}$$

where $C_p = \left\langle \left|\cos\left(2\pi f_c(t-\tau/2)+\theta\right)\right|^{p-2}\right\rangle_t$ is constant. The *p*th-order cyclic correlation of AM signal is expressed as

$$R_{x,p}^{\varepsilon}(\tau) = \begin{cases} \frac{1}{4}C_p e^{\pm i2\theta} R_{a,p}(\tau), & \varepsilon = \pm 2f_c \\ \frac{1}{2}C_p \cos(2\pi f_c\tau) R_{a,p}(\tau), & \varepsilon = 0 \\ 0, & \text{others} \end{cases} \tag{15}$$

Substitution of (15) into (9), the *p*th-order cyclic spectrum is given by

$$S_{x,p}^{\varepsilon}(f) = \begin{cases} \frac{1}{4}C_p e^{\pm i2\theta} S_{a,p}(f), & \varepsilon = \pm 2f_c \\ \frac{1}{4}C_p\left[S_{a,p}(f+f_c) + S_{a,p}(f-f_c)\right], & \varepsilon = 0 \\ 0, & \text{others} \end{cases} \tag{16}$$

In digital phase modulation, the M-PSK signal is represented as

$$x(t) = \sqrt{E_b}\, V_b(t)\exp\{i(2\pi f_c t + \varphi_0)\} \tag{17}$$

where $\sqrt{E_b}$ is the average power, $V_b(t) = \sum_n \varphi_n q(t - nT_d)$, $\varphi_n = e^{i\frac{\pi}{2}(2m-1)}$ ($m = 1,2,...,M$), $q(t)$ is rectangular pulse shape, and T_d is symbol period. We note that the signal $x(t)$ is a BPSK when $m = 1,2$, and it becomes to QPSK signal when $m = 1,2,3,4$. The *p*th-order cyclic spectrum of BPSK signal is

$$S_{x,p}^{\varepsilon}(f)=\begin{cases}\dfrac{E_b^p}{4T_d}\left[Q\left(f+f_c+\dfrac{\varepsilon}{2}\right)Q^*\left(f+f_c-\dfrac{\varepsilon}{2}\right)+Q\left(f-f_c+\dfrac{\varepsilon}{2}\right)Q^*\left(f-f_c-\dfrac{\varepsilon}{2}\right)\right], \varepsilon=\dfrac{n}{T_d} \\ \dfrac{E_b^p}{4T_d}\left[\begin{array}{l} e^{-i2\varphi_0}Q\left(f+f_c+\dfrac{\varepsilon}{2}\right)Q^*\left(f-f_c-\dfrac{\varepsilon}{2}\right)+ \\ e^{i2\varphi_0}Q\left(f-f_c+\dfrac{\varepsilon}{2}\right)Q^*\left(f+f_c-\dfrac{\varepsilon}{2}\right) \end{array}\right], \varepsilon=\pm 2f_c+\dfrac{n}{T_d} \\ 0, \text{ others}\end{cases} \tag{18}$$

where $Q(f)=\dfrac{\sin(\pi fT_d)}{\pi f}$. And the *p*th-order cyclic spectrum of QPSK signal is

$$S_{x,p}^{\varepsilon}(f)=\begin{cases}\dfrac{E_q^p}{4T_d}\left[\begin{array}{l} Q\left(f+f_c+\dfrac{\varepsilon}{2}\right)Q^*\left(f+f_c-\dfrac{\varepsilon}{2}\right) \\ +Q\left(f-f_c+\dfrac{\varepsilon}{2}\right)Q^*\left(f-f_c-\dfrac{\varepsilon}{2}\right) \end{array}\right], \varepsilon=\pm 2f_c+\dfrac{n}{T_d} \\ 0, \text{ others}\end{cases} \tag{19}$$

It can be seen from (16) that the *p*th-order cyclic spectrum of AM signal is not equal to zero only if $\varepsilon=\pm 2f_c$, thus the cycle frequency of AM is $\pm 2f_c$. It indicates that the *p*th-order cyclic spectrum of AM signal in the surface of $f=0$ is not to equal to zero only when $\varepsilon=\pm 2f_c$. It follows from (18) and (19), we see that the *p*th-order cyclic spectra of BPSK and QPSK signals can reach its maximum value at $\varepsilon=\pm 2f_c$ when $f=0$. Thus, $\varepsilon=\pm 2f_c$ is the cycle frequency for AM, BPSK, and QPSK signals. Moreover, the *p*th-order cyclic spectra of AM, BPSK and QPSK signals at $\varepsilon=\pm 2f_c$ are typically stronger than that at other cycle frequencies [5],

$$\left|S_{x,p}^{\pm 2f_c}(0)\right|=\max\{\left|S_{x,p}^{\varepsilon}(0)\right|\} \tag{20}$$

Then the value of the carrier frequency can be obtained by

$$\hat{f}_c=\frac{1}{2}\arg\max_{\varepsilon}\{S_{x,p}^{\varepsilon}(0)\} \tag{21}$$

An advantage of *p*th-order cyclic spectrum over the conventional second-order cyclostationarity is that it takes PFOM with one received signal. This factor can deemphasize the impulsive effects. Since the impulsive noise and interference can be removed by the *p*th-order cyclic statistics, the proposed method is robust and performs well for Gaussian, non-Gaussian $S\alpha S$ noise and cyclostationary interference.

4. Simulation Results

In this section, we present the comparative results on the performance of the new proposed algorithm in various environments. In our simulations, we consider a AM signal, a BPSK signal, and a QPSK signal. Since the α-stable process with infinite variance for $\alpha<2$, we use Generalized signal-to-noise ratio (GSNR) measure as the ratio of the signal power over the impulsive noise dispersion γ ,

$GSNR = 10\log_{10}(E\{|s(t)|^2\}/\gamma)$ [11]. According to this choice of GSNR metric, the $S\alpha S$ noise samples are power scaled by the dispersion parameter γ.

4.1. The p th-Order Cyclic Spectrum

In our first simulation, the carrier frequency of the AM signal is $f_{c1} = 0.2 f_s$. The carrier frequency of the BPSK signal is $f_{c2} = 0.2 f_s$, keying rate $\varepsilon_{k1} = 0.04 / T_s$. The carrier frequency of the QPSK signal is $f_{c3} = 0.1 f_s$, and keying rate $\varepsilon_{k2} = 0.05 / T_s$. The *p*th-order cyclic spectra of AM, BPSK, and QPSK signals are shown in Figure 2, Figure 3 and Figure 4, respectively. Simulation results show that the *p*th-order cyclic statistics has the ability of exploiting the cyclostationarity properties of cyclostationary signals. It is easy to see that the *p*th-order cyclic spectrum surfaces contain two peaks in frequency dimension ($\varepsilon = 0$) corresponding to the frequency $f = \pm f_c$. And it is easy to see that the *p*th-order cyclic spectrum surfaces contain two peaks in cycle frequency dimension ($f = 0$) corresponding to the cycle frequency $\varepsilon = \pm 2 f_c$.

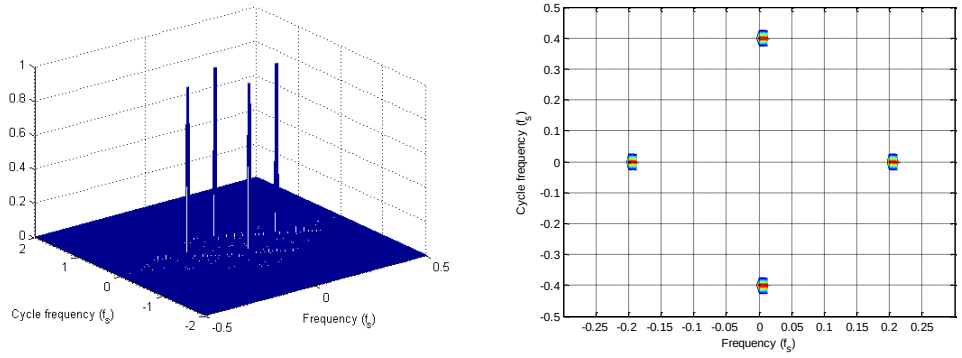

(a) The p th-order Cyclic Spectrum (b) Contour of p th-order Cyclic Spectrum

Figure 2. Calculated p th-order Spectral Correlation Magnitudes for AM Signal

4.2. Effects of Impulsive Noise

In this experiment, we study the effects of impulsive noise on the performance of the conventional and proposed algorithms. The discrete time sampling increment is $T_s = 10^{-6} s$. The carrier frequency of the AM, BPSK, and QPSK is $f_{c1} = 200000$ Hz, $f_{c2} = 200000$ Hz, and $f_{c3} = 100000$Hz, respectively. The characteristic exponent of stable impulsive noise is $\alpha = 1.5$, the $GSNR = -3$ dB, and $p = 1.2$. The cross-sections plots through conventional second-order cyclic spectrum surface in the cycle frequency dimension ($f = 0$) under impulsive noise are shown in Figure 5. Figure 6 shows the cross-sections plots through p th-order cyclic spectrum surface in the cycle frequency dimension ($f = 0$) under impulsive noise.

(a) The p th-order Cyclic Spectrum (b) Contour of p th-order Cyclic Spectrum

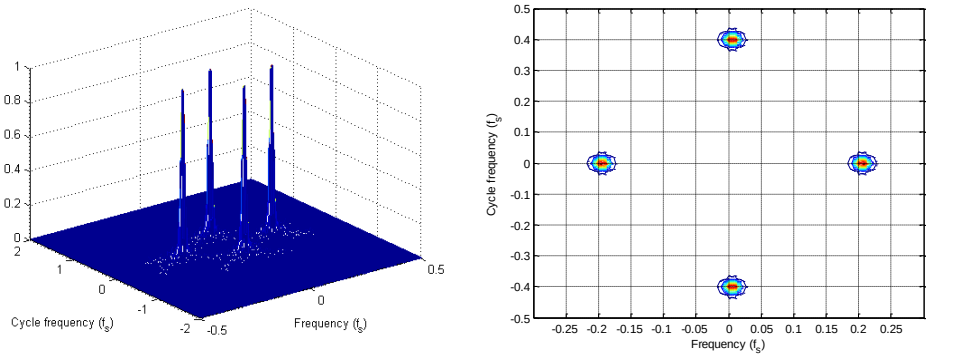

Figure 3. Calculated p th-Order Spectral Correlation Magnitudes for BPSK Signal

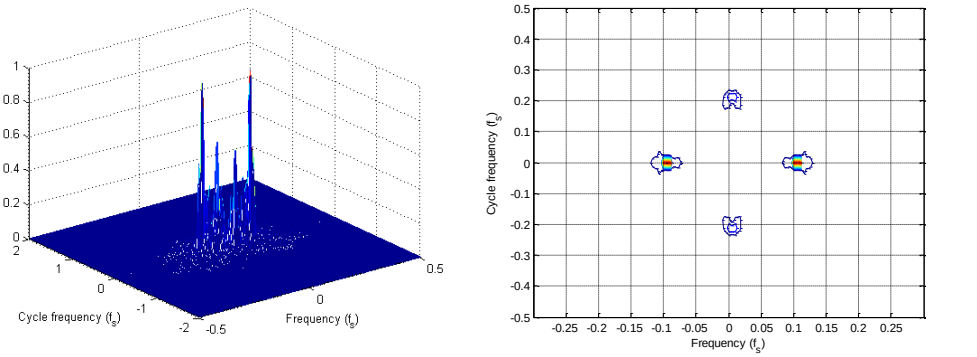

(a) The p th-order cyclic spectrum (b) Contour of p th-order cyclic spectrum

Figure 4. Calculated p th-Order Spectral Correlation Magnitudes for QPSK Signal

The behaviors of the conventional cyclic spectrum degrade severely in stable impulsive noise. We see from Figure 6 that the peak of interest is only one of many peaks, any one of which might be taken as the carrier frequency estimate. In contrast to this, the proposed p th-order cyclic method place clearly distinguished peaks to the carrier frequency in heavy tailed noise, it is more robust than the second-order statistics based algorithm.

4.3. Effects of Impulsive Noise

In this case, the signal is a AM signal with carrier frequency of $f_c = 0.2 / T_s$, the interfering signal is a QPSK signal with carrier frequency of $f_1 = 0.1 / T_s$, keying rate of $\varepsilon_1 = 0.04 / T_s$. The discrete time sampling increment is $T_s = 10^{-6} s$. The signal to interference ratio (SIR) is 3 dB. Figure 7 demonstrates the conventional method based on the DFT and the new proposed method in the presence of interference.

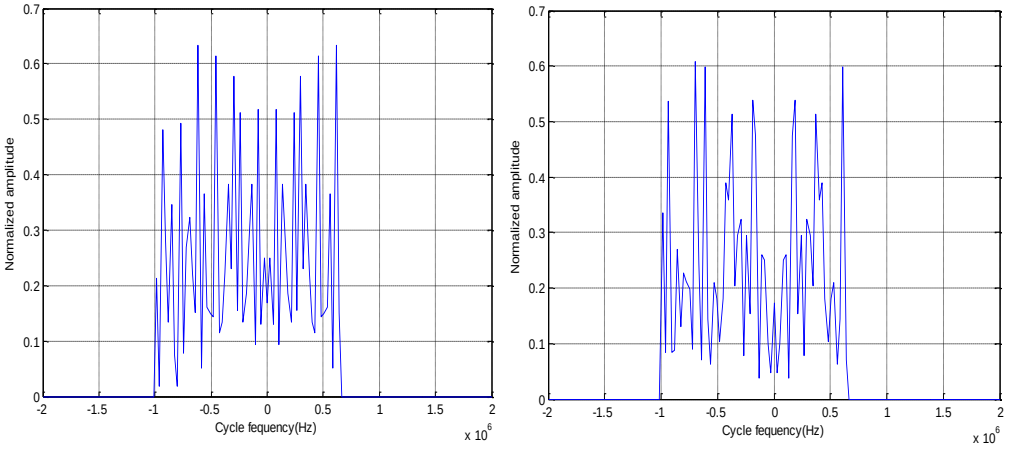

(a) AM Signal (b) BPSK Signal

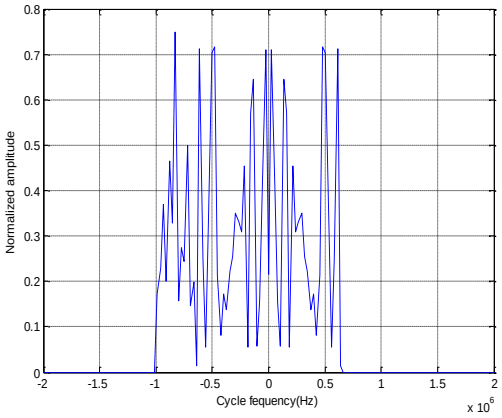

(c) QPSK Signal

Figure 5. Cross-Section Plots through Cyclic Spectrum Surface in the Cycle Frequency Dimension in Impulsive Noise

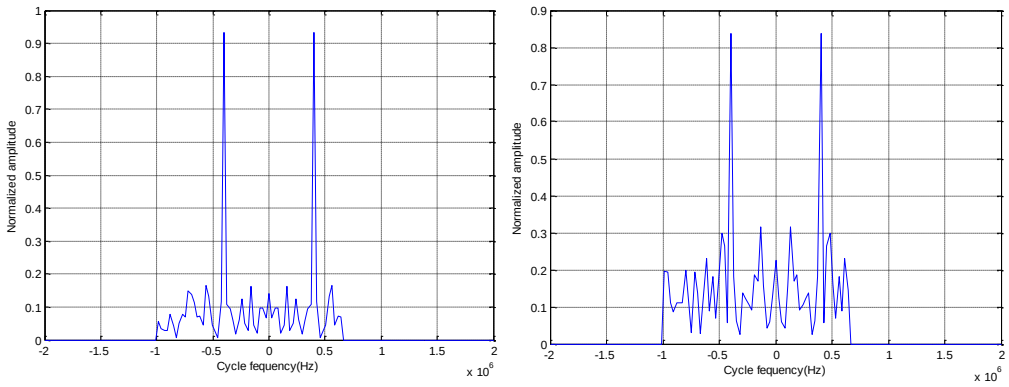

(a) AM Signal (b) BPSK Signal

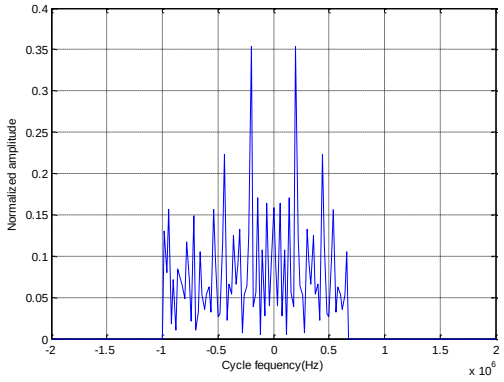

(c) QPSK Signal

Figure 6. Cross-Section Plots through Cyclic Spectrum Surface in the Cycle Frequency Dimension in Impulsive Noise

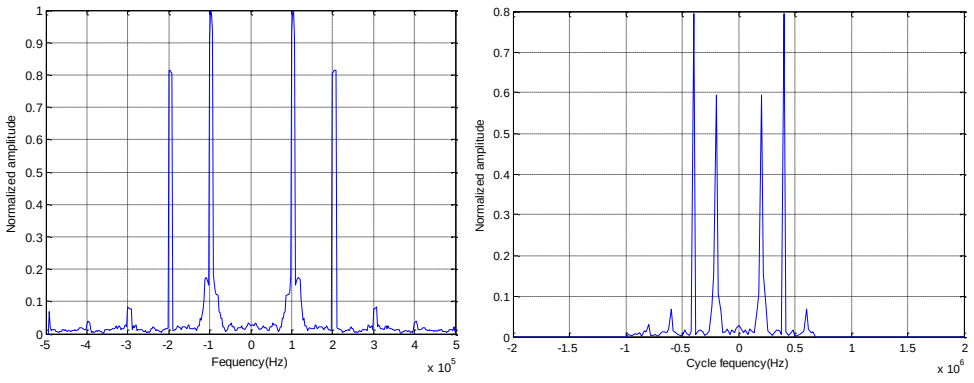

(a) DFT Method (b) Proposed Method

Figure 7. Cross-Section Plots of Conventional DFT Method and the Proposed Method

It can be seen from Figure 7(a) that four peaks occur at the carrier frequency of AM signal ($f = \pm f_c$) and the carrier frequency of interfering QPSK signal ($f = \pm f_1$) for the DFT method. However, the dominant peaks occur at $f = \pm f_1$ which corresponding to the carrier frequency of interfering QPSK signal. Although the DFT method is robust to Gaussian noise, it cannot provide correct estimation results in this case where the interfering signal is present. However, from Figure 7(b) we observe that four peaks occur at $\varepsilon = \pm 2 f_c$ and $\varepsilon = \pm 2 f_1$, the dominant peaks occur at $\varepsilon = \pm 2 f_c$ which corresponding to the carrier frequency of the AM signal. Therefore, the proposed p th-order cyclic spectrum based algorithm is not only robust to impulsive, also immune to the interfering signal.

4.4. Carrier Frequency Estimation

In this section, performance of the proposed method for AM, BPSK, and QPSK signals in Gaussian noise and impulsive noise are analyzed by computer simulations. The discrete time sampling increment is $T_s = 10^{-7} s$. The carrier frequency of AM signal is $f_1 = 0.2 / T_s$. The carrier frequency of BPSK signal is

$f_2 = 0.02 / T_s$, and the keying rate $\varepsilon_1 = 0.005 / T_s$. The carrier frequency of QPSK signal is $f_3 = 0.02 / T_s$, and the keying rate $\varepsilon_2 = 0.005 / T_s$.

In this experiment, the normalized mean square error (NMSE) is used to evaluate the performance of the algorithm. The NMSE is defined as

$$\mathrm{NMSE} = \sum_{i=1}^{N} \left(\hat{f}_i - f_c \right)^2 \Big/ (N f_c^2) \tag{22}$$

where f_c is the carrier frequency of the signal, $\hat{f}_i$ is carrier frequency estimate, and N is Monte Carlo simulation iterations.

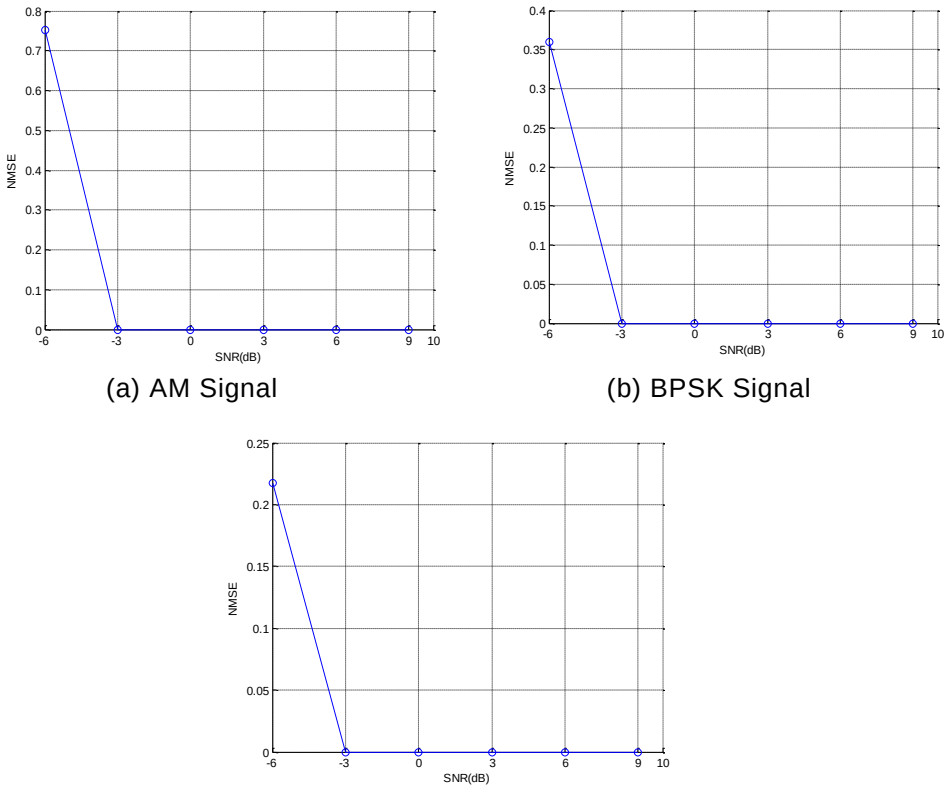

(a) AM Signal (b) BPSK Signal

(c) QPSK Signal

Figure 8. Estimation Accuracy of the Proposed Method in Gaussian Noise

The carrier frequency estimation Normalized mean-squared errors (NMSE) in Gaussian and impulsive noise ($\alpha = 1.7$) are shown in Figure 8 and Figure 9, respectively. It can be seen that the proposed p th-order cyclostationarity based method is insensitive to Gaussian and impulsive noises. We can see from Figure 8 that when the SNR is close to -3 dB the algorithm achieves a steady state. In impulsive noise, the algorithm achieves a steady state when the GSNR is close to 0 dB. Figure 10 shows the estimation results of BPSK signal for the scenarios where slightly ($\alpha = 1.9$) and fairly ($\alpha = 1.5$) impulsive noise are present. Simulation results indicate that the impulsive noise has a more severe impact than the Gaussian noise for the proposed carrier frequency estimation algorithm. Because of the tails of the $S\alpha S$ distribution with $\alpha = 1.5$ is thicker than that of $\alpha = 1.9$, we see from Figure 10 that the overall performance of the proposed method is improved as $\alpha = 1.9$.

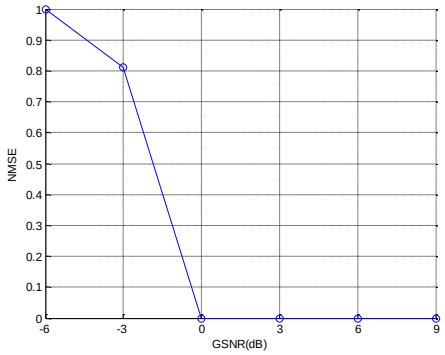

(a) AM Signal

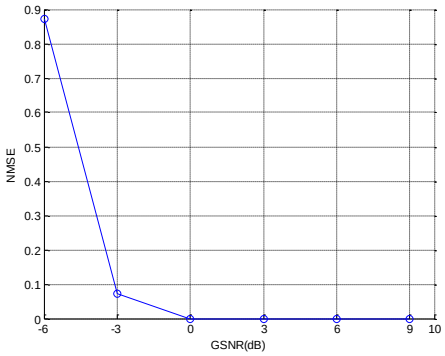

(b) BPSK Signal

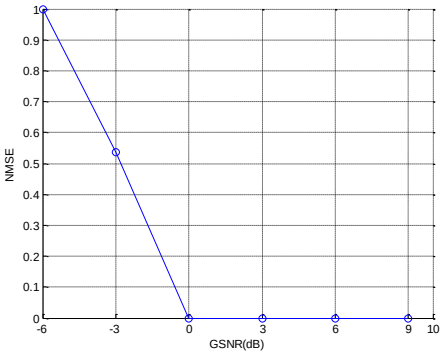

(a) QPSK Signal

Figure 9. Estimation Accuracy of the Proposed Method in Impulsive Noise

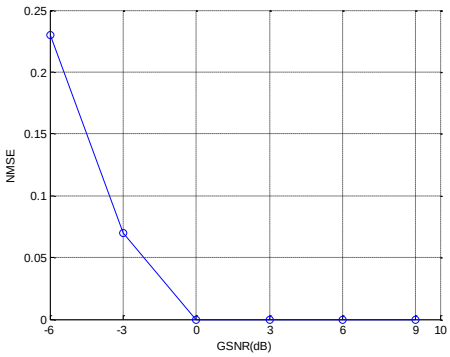

(a) $\alpha = 1.9$

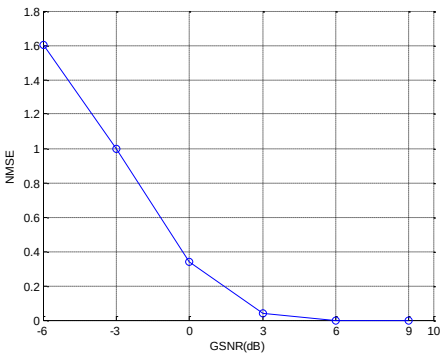

(b) $\alpha = 1.5$

Figure 10. Estimation Accuracy of the Proposed Method for BPSK Signal in Impulsive Noise

5. Conclusions

In this paper, we study carrier frequency estimation method for AM, BPSK, and QPSK cyclostationary signals in the presence of interfering signals and heavy-tailed α-stable impulsive noise. Since the conventional DFT method is degraded in the presence of impulsive noise and interference, the carrier frequency estimation method for AM, BPSK, and QPSK signals is analyzed in this paper. First, a type of representation for revealing the cyclostationarity property of signals using PFLOM operation is developed. Then, a new carrier frequency estimation algorithm based on the p th-order cyclostationarity is proposed. The new method makes better use of the cyclostationarity property and FLOS and is tolerant to interference and impulsive noise. The performance of the proposed method is examined in simulations. Simulation results demonstrate the effectiveness and robustness of the new algorithm. It is shown that the performance of the proposed algorithms is significantly better compared with the conventional estimators in a wide range of interference and noise environments.

Acknowledgments

The authors gratefully acknowledge the financial support provided to this study by the National Science Foundation of China. This work is partly supported by the National Science Foundation of China, under Grants 61362027 and 61461036.

References

[1] M. Morelli and U. Mengali, "Carrier-frequency estimation for transmissions over selective channels", IEEE Transaction on Communications, vol. 48, no. 9, **(2000)**, pp. 1580-1589.
[2] B. Babak and N. A. Reza, "Design and analysis of a reduced phase error digital carrier recovery architecture for high-order quadrature amplitude modulation signals", IET Communications, vol.18, no. 4, **(2010)**, pp. 2196-2207.
[3] C. S. Lee, E. D. Lee and J. M. Ahn, "Fast frequency acquisition algorithm for carrier recovery for high-order QAM", Electronic Letters, vol. 44, no. 2, **(2008)**, pp. 143-144.
[4] D. F. Chen, E. Y. Zhang and J. Zhu, "A fast fourier transform algorithm to estimate carrier frequency deviation", Journal of Circuits and Systems, vol. 11, no. 2, **(2006)**, pp. 128-132.
[5] Q. Wang, Y. Xiao and K. Y. Qin, "Interpolation algorithm for carrier estimation based on DFT in burst M-PSK communication real time multi-domain analysis", Journal of Electronic Science and Technology, vol. 4, no. 2, **(2004)**, pp. 120-126.
[6] W. Kuo and M. P. Fitz, "Frequency offset compensation of pilot symbol assisted modulation in frequency flat fading", IEEE Transaction on Communications, vol. 45, no. 11, **(1997)**, pp. 1412-1426.
[7] V. Lottici, R. Reggiannini and M. Carta, "Pilot-aided carrier frequency estimation for filter-bank multicarrier wireless communications on doubly-selective channels", IEEE Transactions on Signal Processing, vol. 58, no. 5, **(2010)**, pp. 2783-2794.
[8] N. Noels, H. Steendam, M. Moeneclaey and H. Bruneel, "Carrier phase and frequency estimation for pilot-symbol assisted transmission: bounds and algorithms", IEEE Transactions on Signal Processing, vol. 53, no.12, **(2005)**, pp. 4578-4587.
[9] R. F. Brcich, D. R. Iskander and A. M. Zoubir, "The stability test for symmetric alpha-stable distributions", IEEE Transactions on Signal Processing, vol. 53, no. 3, **(2005)**, pp. 977-986.
[10] X. Ma and C. L. Nikias, "Joint estimation of time delay and frequency delay in impulsive noise using fractional lower-order statistics", IEEE Transactions on Signal Processing, vol. 44, no. 11, **(1996)**, pp. 2269-2687.
[11] J. G. Gonzalez, J. L. Paredes and G. R. Arce, "Zero-Order Statistics: a mathematical framework for the processing and characterization of very impulsive signals", IEEE Transactions on Signal Processing, vol. 54, no. 10, **(2006)**, pp. 3839-3851.
[12] S. Zozor, J. M. Brossier and P. O. Amblard, "A parametric approach to suboptical signal detection in alpha stable noise", IEEE Transactions on Signal Processing, vol. 54, no. 12, **(2006)**, pp. 4497-4509.
[13] W. A. Gardner, A. Napolitano and L. Paura, "Cyclostationarity: half a century of research", Signal Processing, vol. 86, no. 4, **(2006)**, pp. 639-697.
[14] A. Napolitano, "Estimation of second-order cross-moments of generalized almost-cyclostationary process", IEEE Transactions on Information Theory, vol. 53, no. 6, **(2007)**, pp. 2204-2228.

[15] M. R. Morelande and A. M. Zoubir, "On the performance of cyclic moment based parameter estimators of amplitude modulated polynomial phase signals", IEEE Transactions on Signal Processing, vol. 50, no.3, **(2002)**, pp. 590-605.

Authors

Yang Liu received the B.Eng. degree from the Inner Mongolia University and the Ph.D. degree from the Dalian University of Technology, both in electronic engineering, in 2003 and 2012, respectively. He is currently an Associate Professor with the College of Electronic Information Engineering, Inner Mongolia University, China. His research interests include parameter estimation, non-Gaussian signal processing, and array signal processing.

Yong Tie received the B.Eng. degree from the Inner Mongolia University in electronic engineering, in 1985. He is currently a Professor with the College of Electronic Information Engineering, Inner Mongolia University, China. His research interests include signal detection and parameter estimation, DSP application.

